

AE 721 Report 10

105mm RAIDER Weapon System Design

Written by Joseph Ative, Payton Kuligowski, Joshua Poznanski, Jakob Richardson, Cade Schneider, and Hector Torres

December 4th, 2023

Table of Contents

	Page No.
List of Figures.....	iii
List of Tables	iv
List of Symbols.....	v
Acknowledgements.....	vii
1 105mm RAIDER Background.....	1
2 105mm RAIDER Powerplant Layout.....	3
3 Flight Assumptions and Mission Profile	4
4 105mm RAIDER Powerplant Design for Mach 4 at Apogee/Cruise Initiation Point.....	5
4.1 Determination of T_{req} at CIP	5
4.2 Assumptions	5
4.3 Calculation of A_0 and A_{IT}	5
4.4 Calculation of M_3 , M_4 , and P_4	6
4.5 Calculation of a_4	6
4.6 Calculation of V_4	6
4.7 Calculation of L_c	7
4.8 Determination of A_t	7
4.9 Design of Nozzle.....	7
4.10 Determine Engine Thrust and Specific Impulse	8
5 Design Iteration and Optimization	9
5.1 Iteration I.....	9
5.2 Iteration II.....	9
5.3 Iteration III	10
5.4 Iteration IV	11
5.5 Iteration V	11
6 Final RAIDER Weapon CAD Figures	13
6.1 Fully Collapsed/Stowed	13
6.2 Post Launch/Burnout.....	15
6.3 Dash/Terminal Flight	18
7 Conclusions and Recommendations.....	22
7.1 Summary	22

7.2	Recommendations	23
7.3	Section Responsibilities	23
	References	24
	Appendix A: Calculation of Apogee Altitude	A-1

List of Figures

	Page No.
Figure 1.1: The Authors with the 105mm RAIDER Model	2
Figure 2.1: 105mm RAIDER Powerplant Internal Schematic.....	3
Figure 3.1: Example Mission Profile of 105mm RAIDER (Ref. 3, Ref. 4)	4
Figure 4.1: Theoretical Nozzle Design for the 105mm RAIDER	7
Figure 6.1: Isometric View of the 105mm RAIDER in the Pre-Launch Configuration.....	13
Figure 6.2: Front View of the 105mm RAIDER in the Pre-Launch Configuration	14
Figure 6.3: Side View of the 105mm RAIDER in the Pre-Launch Configuration.....	14
Figure 6.4: Isometric View of the 105mm RAIDER in the Pre-Launch Configuration.....	14
Figure 6.5: Isometric Cutaway View of the 105mm RAIDER in the Pre-Launch Configuration	15
Figure 6.6: Isometric View of the 105mm RAIDER in the Post-Launch Configuration	16
Figure 6.7: Front View of the 105mm RAIDER in the Post-Launch Configuration.....	16
Figure 6.8: Side View of the 105mm RAIDER in the Post-Launch Configuration	17
Figure 6.9: Top View of the 105mm RAIDER in the Post-Launch Configuration	17
Figure 6.10: Isometric Cutaway View of the 105mm RAIDER in the Post-Launch Configuration	18
Figure 6.11: Isometric View of the 105mm RAIDER in the Terminal Configuration.....	19
Figure 6.12: Front View of the 105mm RAIDER in the Terminal Configuration	19
Figure 6.13: Side of the 105mm RAIDER in the Terminal Configuration	20
Figure 6.14: Top View of the 105mm RAIDER in the Terminal Configuration	20
Figure 6.15: Isometric Cutaway View of the 105mm RAIDER in the Terminal Configuration..	21

List of Tables

Page No.

Table I: Performance Characteristic Comparison (Ref. 1)	1
---	---

List of Symbols

<u>Symbol</u>	<u>Definition</u>	<u>Units</u>
A_0	Inlet Area	in^2 (m^2)
a_4	Exit Speed of Sound	ft/s (m/s)
A_{IT}	Inlet Throat Area	in^2 (m^2)
A_t	Throat Area	in^2 (m^2)
c^*	Characteristic Velocity	ft/s (m/s)
d	Diameter	in (m)
g	Gravitational Acceleration	ft/s^2 (m/s^2)
I_{sp}	Specific Impulse	s
L_c	Chamber Length	~
m	Mass	lbm (kg)
M	Mach Number	~
\dot{m}	Mass flow rate	lbs/s (kg/s)
M_0	Free Stream Mach Number	~
M_3	Inlet Mach	~
M_4	Exit Mach	~
M_{IE}	Inlet Entrance Mach Number	~
\dot{m}_{tot}	Total Mass Flow Rate	lbs/s (kg/s)
P_4	Exit Pressure	psf (Pa)
R	Range	ft (m)
S	Surface Area	ft^2 (m^2)
t	Time	seconds (s)
T_3	Combustor Entrance Temperature	$^{\circ}\text{R}$ (K)
T_4	Combustor Exit Temperature	$^{\circ}\text{R}$ (K)
T_{req}	Required Thrust Force	lbf (N)
V_4	Combustor Exit Flow Velocity	ft/s (m/s)

Greek Symbols

<u>Symbol</u>	<u>Definition</u>	<u>Units</u>
α	Angle of Attack	degrees ($^{\circ}$)
γ	Ratio of Specific Heats	~

Subscripts

<u>Symbol</u>	<u>Definition</u>	<u>Units</u>
0	Inlet	~
3	Combustor Entrance	~
4	Combustor Exit	~
IE	Inlet Entrance	~
IT	Inlet throat	~
max	Maximum	~
req	Required	~
t	Throat	~
tot	Total	~

Acronyms**Definition****Units**

AOA	Angle of Attack	Degrees (°)
CAD	Computer Aided Design	~
HERA	High-Explosive Rocket-Assisted	~
OML	Outer Mold Line	~
PE	Potential Energy	ft-lb (J)
RAIDER	Ram Air Inflated Duct Eccentric Ramjet	~
SOTA	State of the Art	~

Acknowledgements

The authors would like to thank Lucas Russell and Jeb “Jeeb” Marshal for helping. Additionally, the authors would like to thank Duck Carson for providing emotional support and help debugging code.

1 105mm RAIDER Background

The objective of this chapter is to summarize the results determined in previous technical reports on the RAIDER configuration of 105mm artillery shells. Technical details come from Ref. 1.

The objective of the 105mm Ram Air Inflated Duct Eccentric Ramjet (RAIDER) configuration is to increase the range of conventional 105mm rounds compared to state of the art (SOTA) systems like the M927 HERA (High Explosive Rocket Assisted) projectiles. To develop the design characteristics of the RAIDER projectile, the authors calculated aerodynamic, performance, and salient characteristics of the M927 HERA and a scaled estimate of the Boeing-NAMMO 155mm ramjet projectile. The geometric characteristics of the 105mm RAIDER derived from these systems is provided in Table I.

Table I: 105mm RAIDER Geometric Characteristics (Ref. 1)

Characteristic	Measurement
Projectile Length	24.212 in.
Nose Length	12.441 in.
Nose Diameter	0.039 in.
Fin Mean Aerodynamic Chord	0.228 in.
Fin Total Surface Area	0.236 in.
Fin Leading Edge Sweep Angle	56.3 deg
Mean Aerodynamic Chord Thickness	0.091 in.
Wingspan Fin	3.937 in.
Leading Edge Section Angle	2 deg

These systems were then reversed engineered using available open-source information and analytical techniques to determine estimated propulsion and ballistic performance. Using this data, the 105mm RAIDER was proverse engineered to deliver marked improvements compared to the baseline systems. Table II displays the benchmark values compared to the newly designed initial RAIDER configuration.

Table II: Performance Characteristic Comparison (Ref. 1)

Characteristic	Benchmark System	RAIDER Configuration	Percent Change
Specific Impulse (s)	400	1300	+ 225%
Thrust (N)	44	88	+ 100%
Range (km)	25	81	+ 224%

Additional changes include an increase in nose fineness ratio by 65% and an increase in normal force generation by 60%. Both characteristics promote reduced drag and therefore increased range. It is important to note that this design does not make use of a forward control surface like canards, which reduces control authority in flight and reduces terminal precision. The authors elected to pursue a configuration designed solely for maximum range performance, and subsequent iterations will feature canards or other forward controls to increase terminal precision. The current fin configuration allows the projectile to stabilize after leaving the barrel and leverage the inflated ducts as a lifting body, capitalizing on optimal lift to drag ratio in that flight configuration. The newly designed 105mm RAIDER was then created as a scale mockup and presented to industry and government professionals at the NDIA Air Armament Symposium. Figure 1.1 showcases the authors along with the model projectile.



Figure 1.1: The Authors with the 105mm RAIDER Model

The content to follow in this report will detail the configuration and resizing of the projectile based on necessary ramjet powerplant requirements. Dimensions for critical locations within the engine will be determined and a new configuration will be developed for further iteration in subsequent reports.

2 105mm RAIDER Powerplant Layout

Figure 2.1 illustrates a breakdown of the 105mm RAIDER powerplant layout.

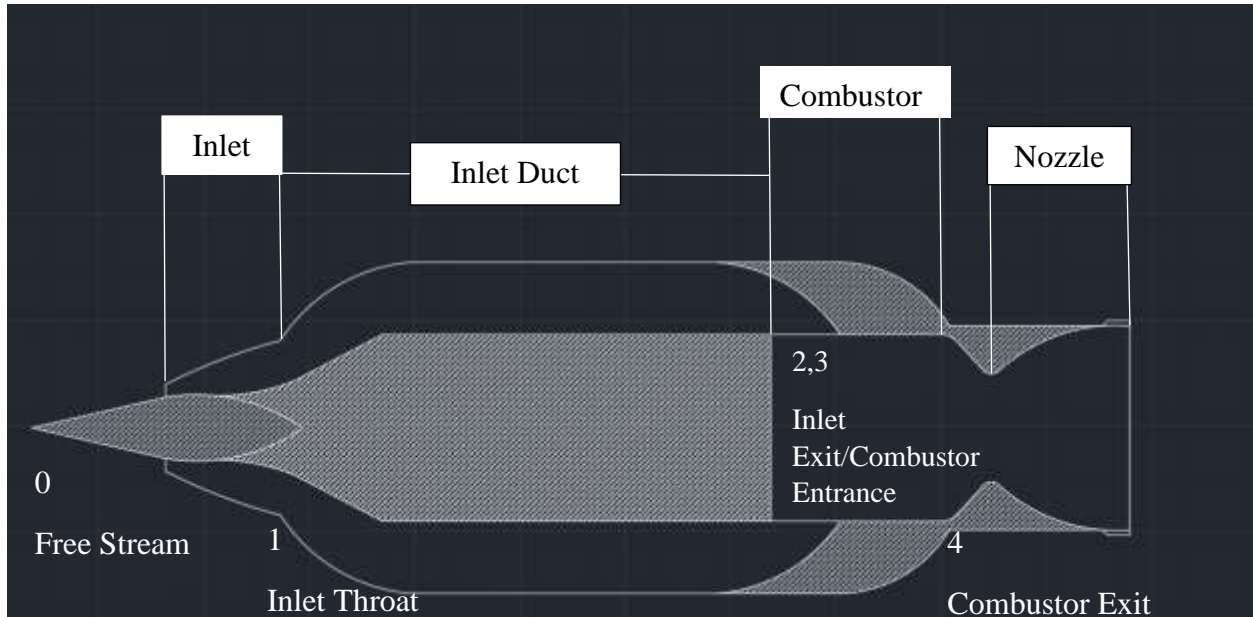


Figure 2.1: 105mm RAIDER Powerplant Internal Schematic

3 Flight Assumptions and Mission Profile

The objective of this chapter is to determine the maximum flight altitude of the 105mm RAIDER powerplant considering a velocity of Mach 4 apogee.

To simplify the calculation of the apogee altitude, several assumptions will be made. These assumptions are summarized in the following list:

- The projectile will have a muzzle velocity of Mach 7, fired from a static position at sea level,
- Kinetic energy will be traded for potential energy, with the projectile experiencing a 50% loss in kinetic energy by the time it reaches apogee,
- Flight velocity at apogee will be Mach 4.

An example mission profile for the 105mm RAIDER round can be seen in Figure 3.1 below. The apogee altitude was found to be $h \cong 160,000ft$. The calculations for this altitude can be seen in Appendix A.

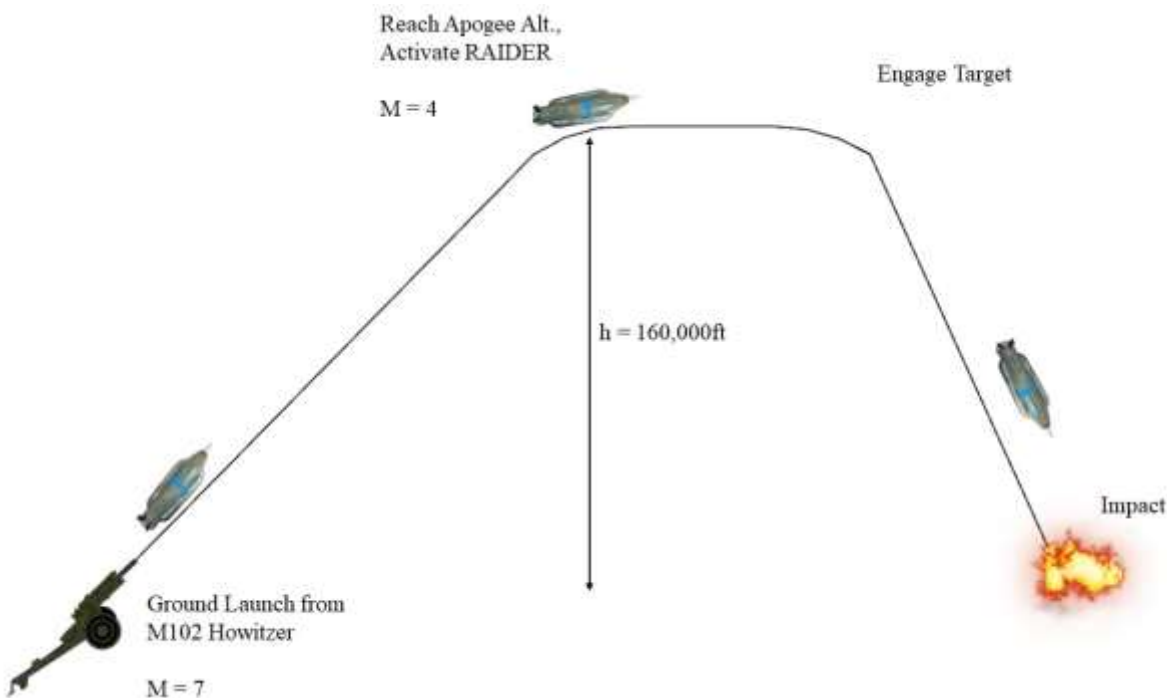


Figure 3.1: Example Mission Profile of 105mm RAIDER (Ref. 3, Ref. 4)

4 105mm RAIDER Powerplant Design for Mach 4 at Apogee/Cruise Initiation Point

The objective of this chapter is to optimally design the 105mm RAIDER powerplant based on the conditions outlined in Chapter 3. These characteristics will be estimated using the methods and approaches defined in Eugene Fleeman's *Missile Design and System Engineering* (Ref. 2).

4.1 Determination of T_{req} at CIP

From previous work, the normal force coefficient of the raider projectile at 5-degree AOA is 0.758. The projectile, traveling Mach 4 at an altitude of 160,000 ft, experiences about 3 lbf of drag. To maintain cruise conditions, the required thrust (T_{req}) must equal the 3 lbf drag force.

4.2 Assumptions

To simplify the calculations made for the first design iteration, the following basic assumptions concerning relevant areas, pressures, and temperatures were made.

- Air below 800 °R behaves as a calorically perfect gas.
- Isentropic flow through the inlet, RAIDER ducts, and nozzle.
- Constant pressure combustion
- Perfectly expanded flow exiting the nozzle.

4.3 Calculation of A_0 and A_{IT}

The objective of this section is to calculate inlet area (A_0) and inlet throat area (A_{IT}). To simplify the calculation of these values, the following assumptions are made:

- The fuel-air ratio is initially stoichiometric,
- If the calculated A_0 is larger than the major area of the projectile, assume instead that they are equal,
- Inlet start Mach number (M_{IE}) is 1.5,
- The inlet is a quasi-isentropic compression spike.

The required A_0 to maintain a Mach 4 cruise at 70,000ft is 8.5 in². The projectile only has 13 in² of frontal area therefore the design is still feasible. A_{IT} is calculated to be 11 in² from Equation 4.1.

$$A_{IT} = A_0 * 1.728 * M_{IE} * (1 + 0.2 * M_{IE}^2)^{-3} \quad (Eq. 4.1)$$

4.4 Calculation of M_3 , M_4 , and P_4

The objective of this section is to calculate the combustor inlet Mach number (M_3), exit Mach number (M_4), and exit pressure (P_4). To simplify the calculation of these values, the following assumptions are made:

- Using Figure 3.30 and $M_0 = 4$, $T_4/T_0 = 12$
- From Figure 3.31, the estimated M_3 is 0.3.

Following the steps and equations laid out in Ref. 2, M_4 and P_4 are calculated.

$$a = 1.822 * \frac{T_4}{T_3} * M_3^2 - 1.175 = -0.7$$

$$b = 2.7 * \frac{T_4}{T_3} * M_3^2 = 0.7$$

$$c = \frac{T_4}{T_3} * M_3^2 = 0.26$$

$$M_4 = \left(\frac{-b - (b^2 - 4 * a * c)^{0.5}}{2 * a} \right)^{0.5} = 1.14$$

$$P_3 = P_0 * \left(1 + \frac{\gamma_0 - 1}{2} * M_0^2 \right)^{\frac{\gamma_0}{\gamma_0 - 1}} = 4 \text{ psi}$$

$$P_4 = P_3 * \frac{\left(1 + \frac{\gamma_0 - 1}{2} * M_4^2 \right)^{\frac{\gamma_0}{\gamma_0 - 1}}}{1 + \gamma_0 * M_4^2} = 3 \text{ psi}$$

4.5 Calculation of a_4

The objective of this section is to calculate the speed of sound in the combustion chamber (a_4). To simplify the calculation of this value, the ratio of specific heats (γ) is estimated to be 1.3 and the exit temperature (T_4) is 5600 °R.

$$a_4 = \sqrt{1.3 * 1545 * T_4} = 3400 \frac{ft}{s}$$

4.6 Calculation of V_4

The objective of this section is to calculate the velocity of combustion (V_4) using values from the prior two sections.

$$v_4 = M_4 * a_4 = 3800 \frac{ft}{s}$$

4.7 Calculation of L_c

The objective of this section is to calculate the combustion chamber length (L_c) using V_4 and a combustion time t_{comb} of 0.001 s as defined in Ref. 2.

$$L_c = t_{comb} * v_4 = 3.8 \text{ ft}$$

4.8 Determination of A_t

The objective of this section is to determine the throat area (A_t) using P_4 and Figure 3.53 from Ref. 2. The total mass flow rate (\dot{m}_{tot}) is estimated to be 0.07 lbm/s, and no spillage is assumed. The characteristic velocity (c^*) is assumed to be 5200 ft/s.

$$A_t = \dot{m}_{tot} * \frac{c^*}{g * P_4} = 0.5 \text{ in}^2$$

4.9 Design of Nozzle

The objective of this section is to design a theoretical nozzle for the 105mm RAIDER powerplant, assuming the nozzle extends to the outer mold line (OML) of the projectile.



Figure 4.1: Theoretical Nozzle Design for the 105mm RAIDER

4.10 Determine Engine Thrust and Specific Impulse

The objective of this subsection is to determine the thrust of the RAIDER powerplant and corresponding specific impulse based on the above calculations.

The following equations are used to calculate the ramjet thrust and I_{sp} at the previously mentioned conditions. Thrust is found to be 3 lbf and I_{sp} is 256 s. The specific impulse is found to be much lower than the initially assumed value of 1300s. This means less fuel can be carried than initially estimated.

$$\frac{T}{A_0 p_0} = \gamma_0 * M_0^2 * \left[\left(\frac{\frac{T_4}{T_0}}{1 + \left(\frac{\gamma_0 - 1}{2}\right) * M_0^2} \right)^{0.5} - 1 \right]$$

$$T_{req} = \frac{T}{A_0 p_0} * A_0 * p_0$$

$$I_{sp} = cd * \left(\left(2 * \frac{\gamma_0^2}{\gamma_0 - 1} \right) * \left(\frac{2}{\gamma_0 + 1} \right)^{\frac{\gamma_0 + 1}{\gamma_0 - 1}} * \left(1 - \left(\frac{p_0}{p_3} \right)^{\frac{\gamma_0 - 1}{\gamma_0}} \right) \right)^{0.5} + \frac{p_0}{p_3} * \frac{A_e}{A_t} - \frac{p_0}{p_3} * \frac{A_e}{A_t} * \frac{c^*}{32.2}$$

5 Design Iteration and Optimization

The objective of this chapter is to optimize the design detailed in Chapter 4 by minimizing complexity, weight, cost, and specific impulse. Five total iterations were performed.

5.1 Iteration I

The first iteration utilizes the characteristics calculated in Chapter 4. These characteristics are tabulated below in Table III.

Table III: Iteration I Characteristics

Characteristic	Measurement
A_0	13 in ²
A_{Γ}	11 in ²
A_3	24 in ²
A_t	0.72 in ²
A_e	11.6 in ²
L_c	3.8 ft
T_4/T_0	11.7
H_f	17900 BTU/lbm
V_{fuel}	36 in ³
T	4.6 lbf
T/D	1.6
Isp	256

The most notable of the characteristics above is the length of the combustion chamber, which expands past the OML of the projectile if left straight. To design a combustor with the required combustion length, a helix pattern was utilized. The helix extends the length of combustion to the needed length without the need for elongation of the projectile.

5.2 Iteration II

The second iteration was designed to reduce the thrust to drag ratio down to 1, as needed for cruise flight. To achieve this condition, the inlet area, and consequently all the other areas, were reduced. The characteristics and changes made to this iteration are displayed in Table IV.

Table IV: Iteration II Characteristics

Characteristic	Measurement	% Change
A_0	8.5 in ²	- 35%
A_{IT}	7.2 in ²	- 35%
A_3	15.8 in ²	- 34%
A_t	0.5 in ²	- 31%
A_e	7.5 in ²	- 35%
L_c	3.8 ft	0%
T_4 / T_0	11.7	0%
H_f	17900 BTU/lbm	0%
V_{fuel}	24 in ³	- 33%
T	3 lbf	- 35%
T/D	1	- 38%
I_{sp}	256	0%

While all the areas changed due to the inlet area changes, the combustor was unaltered. The reduction in weight comes primarily from the decreased fuel volume present in the projectile, which was reduced quite significantly from prior iterations.

5.3 Iteration III

For the third iteration, the areas were enlarged slightly, and the combustor temperature ratio was lowered. The objective of these changes was to decrease the combustor length, which was accomplished. The changes to this iteration are shown in Table V.

Table V: Iteration III Characteristics

Characteristic	Measurement	% Change
A_0	13 in ²	+ 53%
A_{IT}	11 in ²	+ 53%
A_3	20.5 in ²	+ 30%
A_t	0.5 in ²	0%
A_e	7.2 in ²	- 4%
L_c	3.1 ft	- 18%
T_4 / T_0	8	- 32%
H_f	17900 BTU/lbm	0%
V_{fuel}	22 in ³	- 8%
T	2.9 lbf	- 3%
T/D	1	0%
I_{sp}	256	0%

The combustor length changes also corresponded with a decrease in fuel volume and exit area, with a minor penalty to thrust. This penalty is offset by a decrease in drag, maintaining a thrust to drag ratio of 1. Decreases in weight due to the combustor length and fuel volume changes aid in increasing projectile performance.

5.4 Iteration IV

Changes to the fourth iteration continued with reduction of combustor temperature ratio without altering the inlet areas, further reducing the combustor length. The changes to this iteration are shown in Table VI.

Table VI: Iteration IV Characteristics

Characteristic	Measurement	% Change
A_0	13 in ²	0%
A_{IT}	11 in ²	0%
A_3	18 in ²	- 12%
A_t	0.28 in ²	- 44%
A_e	4.5 in ²	- 38%
L_c	2.7 ft	- 13%
T_4 / T_0	6	- 25%
H_f	17900 BTU/lbm	0%
V_{fuel}	14 in ³	- 36%
T	1.8 lbf	- 38%
T/D	0.6	- 40%
I_{sp}	256	0%

The changes in this iteration drastically reduced the weight by minimizing combustor length and fuel volume. However, these changes came at the expense of drastically decreased thrust, so the point that the projectile no longer maintained a thrust to drag ratio of 1. The new changes from this iteration are shown in Figure 5.4.

5.5 Iteration V

The changes made for the fifth and final iteration were made to remedy the issues with the thrust to drag ratio of the previous iteration. These changes took the form of decreasing inlet areas and increasing combustor length. The characteristics of the final iteration are listed in Table VII.

Table VII: Iteration V Characteristics

Characteristic	Measurement	% Change
A ₀	8 in ²	- 38%
A _{IT}	6.8 in ²	- 38%
A ₃	15 in ²	- 17%
A _t	0.45 in ²	+ 61%
A _e	7.1 in ²	+ 58%
L _c	3.8ft	+ 41%
T ₄ /T ₀	11.7	+ 95%
H _f	17900 BTU/lbm	0%
V _{fuel}	22 in ³	+ 57%
T	2.8 lbf	+ 56%
T/D	1	+ 66%
Isp	256	0%

The impact of the changes made to the final iteration are reminiscent of earlier iterations, in that the combustor length is now longer and the combustor temperature ratio is quite high. Fuel volume has also increased, meaning weight is also substantially increased compared to the prior iteration. The increase in thrust offsets this penalty, and the return of a thrust to drag ratio of 1 is critical.

For the sake of time and brevity, the characteristic values of the 105mm RAIDER will not be iterated to closure, and the fifth iteration will be utilized to model the projectile in the following chapter.

6 Final RAIDER Weapon CAD Figures

The objective of this chapter is to display and discuss three configurations of the 105mm RAIDER projectile using CAD modeling. The three configurations to be discussed are:

- i. Fully Collapsed/Stowed: Pre-Launch Configuration, all motors and surfaces stowed,
- ii. Post Launch/Burn Out: Rocket motor expended, ducts and control surfaces stowed,
- iii. Dash/Terminal Flight: RAIDER ducts inflated, and control surfaces deployed.

6.1 Fully Collapsed/Stowed

The objective of this section is to display the 105mm RAIDER in its pre-launch configuration. The RAIDER ducts and control surfaces are stowed, and the projectile is preparing to be launched using a solid fuel rocket booster that fills the combustion chamber of the ramjet engine. Figure 6.1 displays an isometric view of the projectile in this configuration.

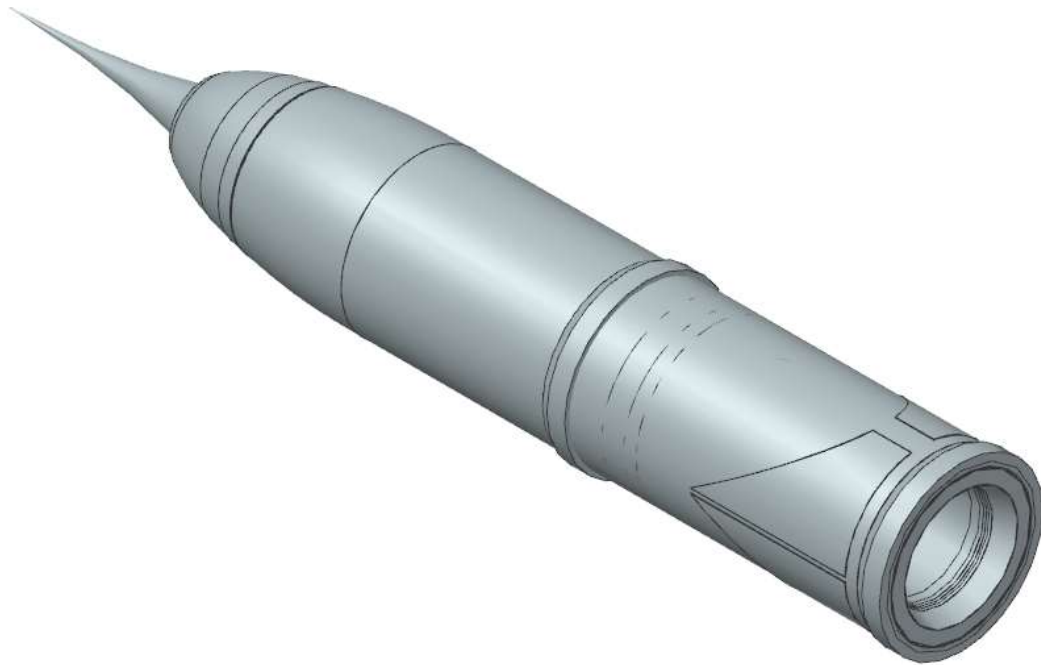


Figure 6.1: Isometric View of the 105mm RAIDER in the Pre-Launch Configuration

Figures 6.2, 6.3, and 6.4 display the front, side, and top views of the projectile in this configuration respectively.



Figure 6.2: Front View of the 105mm RAIDER in the Pre-Launch Configuration



Figure 6.3: Side View of the 105mm RAIDER in the Pre-Launch Configuration



Figure 6.4: Isometric View of the 105mm RAIDER in the Pre-Launch Configuration

Figure 6.5 shows a cutaway view of the internals of the projectile in this configuration. Key details are labeled, including closed ducts and control surfaces, as well as the rocket motor.

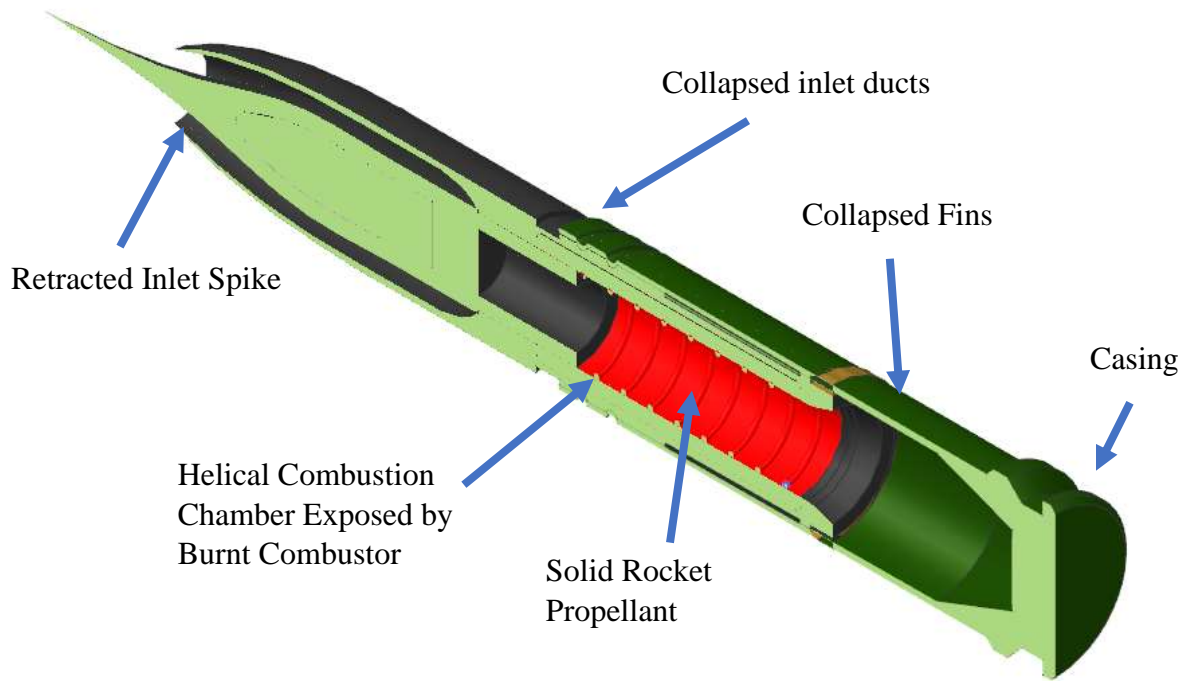


Figure 6.5: Isometric Cutaway View of the 105mm RAIDER in the Pre-Launch Configuration

6.2 Post Launch/Burnout

The objective of this section is to display the 105mm RAIDER in its after launch and burnout configuration. The RAIDER ducts and control surfaces are still stowed, and the projectile has utilized the rocket booster that within the combustor to get to the apogee of the system. Figure 6.6 displays an isometric view of the projectile in this configuration.

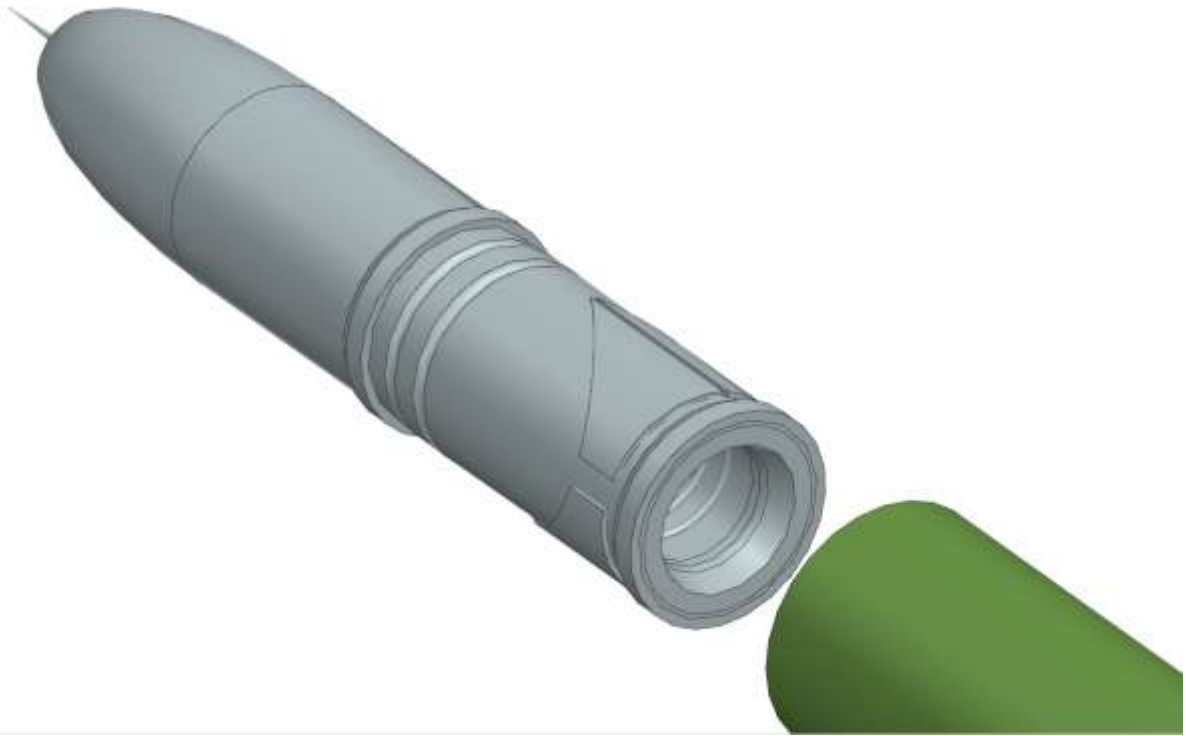


Figure 6.6: Isometric View of the 105mm RAIDER in the Post-Launch Configuration

Figures 6.7, 6.8, and 6.9 display the front, side, and top views of the projectile in this configuration respectively.



Figure 6.7: Front View of the 105mm RAIDER in the Post-Launch Configuration



Figure 6.8: Side View of the 105mm RAIDER in the Post-Launch Configuration



Figure 6.9: Top View of the 105mm RAIDER in the Post-Launch Configuration

Figure 6.10 shows a cutaway view of the internals of the projectile in this configuration. Key details are labeled, including closed ducts and control surfaces, and the newly exposed ramjet combustion chamber in place of the now burned out solid rocket motor.

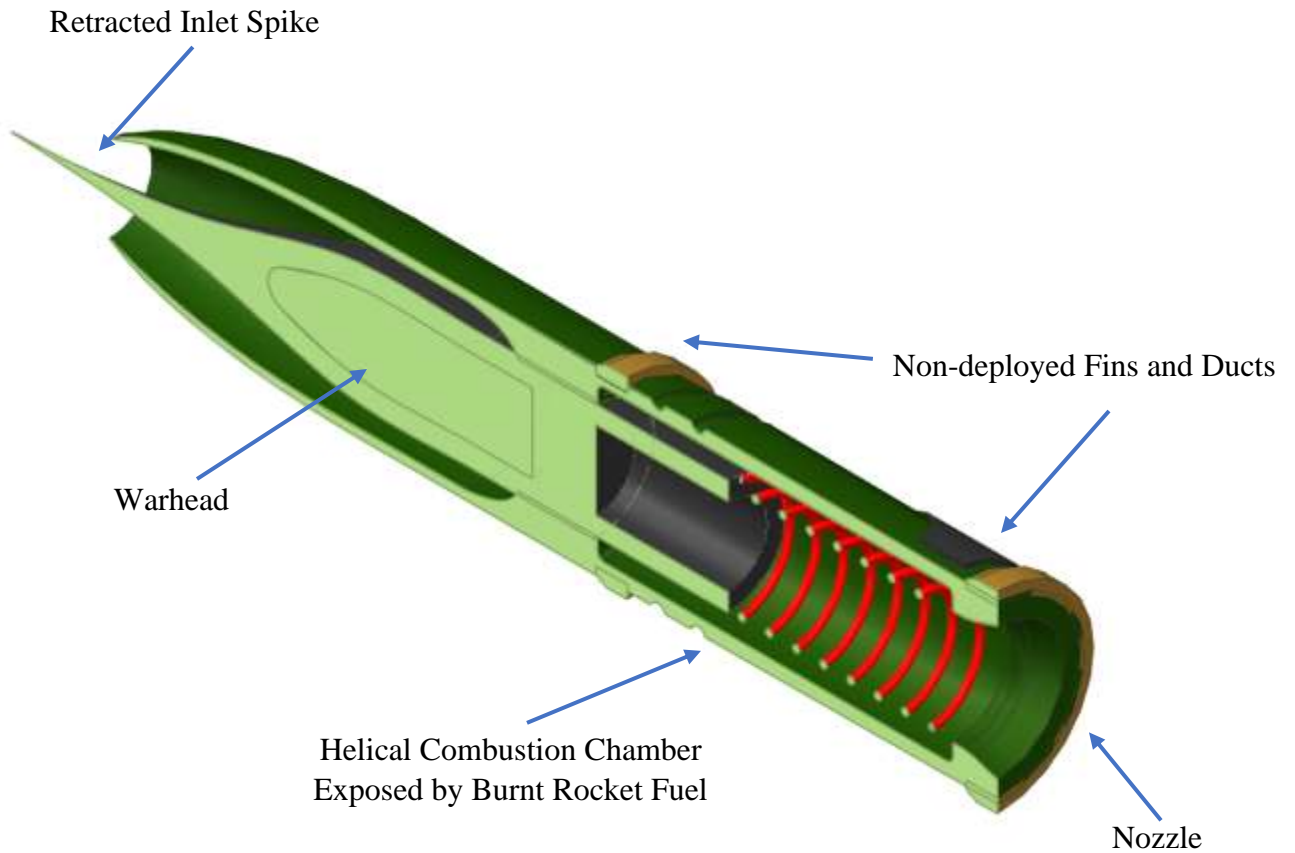


Figure 6.10: Isometric Cutaway View of the 105mm RAIDER in the Post-Launch Configuration

6.3 Dash/Terminal Flight

The objective of this section is to display the 105mm RAIDER in its dash and terminal flight configuration. The RAIDER ducts and control surfaces are deployed, and the projectile has made use of the ramjet engine to propel itself towards the target. Figure 6.11 displays an isometric view of the projectile in this configuration.

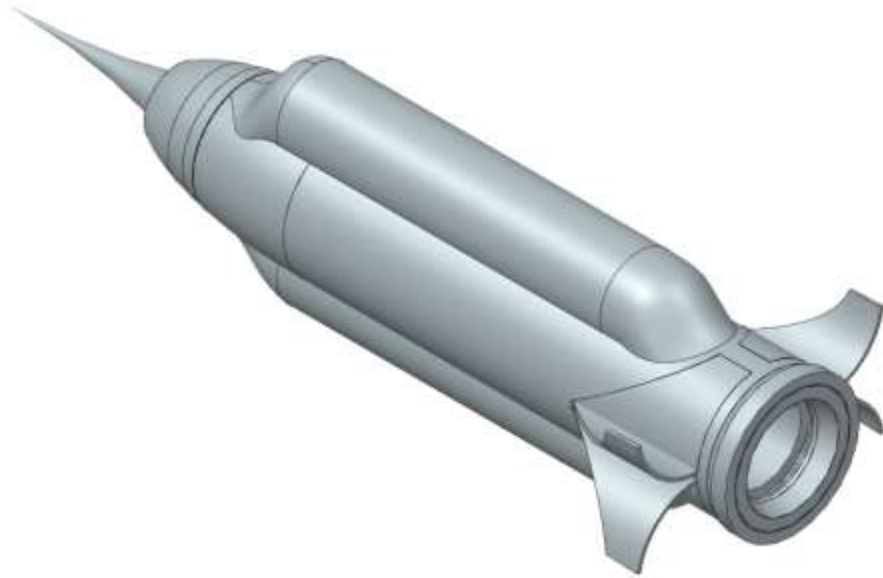


Figure 6.11: Isometric View of the 105mm RAIDER in the Terminal Configuration

Figures 6.12, 6.13, and 6.14 display the front, side, and top views of the projectile in this configuration respectively.

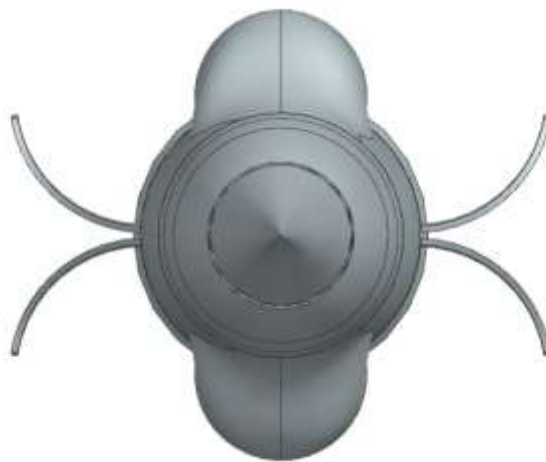


Figure 6.12: Front View of the 105mm RAIDER in the Terminal Configuration

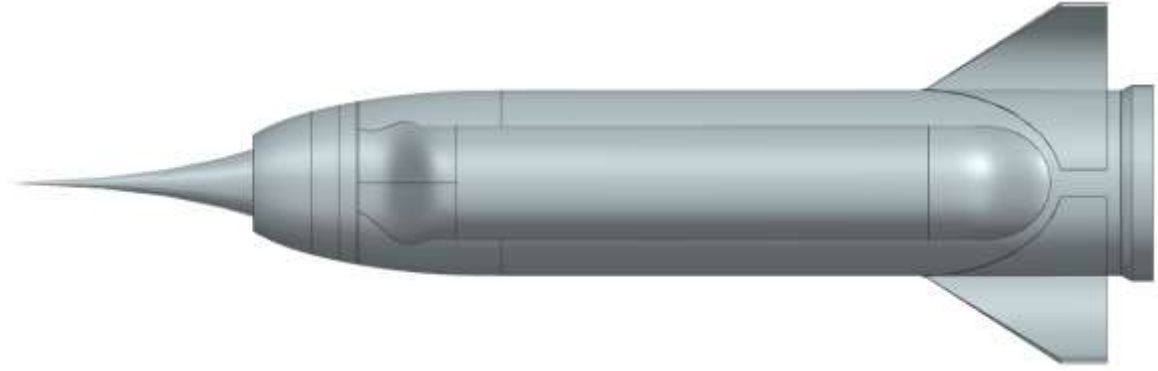


Figure 6.13: Side of the 105mm RAIDER in the Terminal Configuration

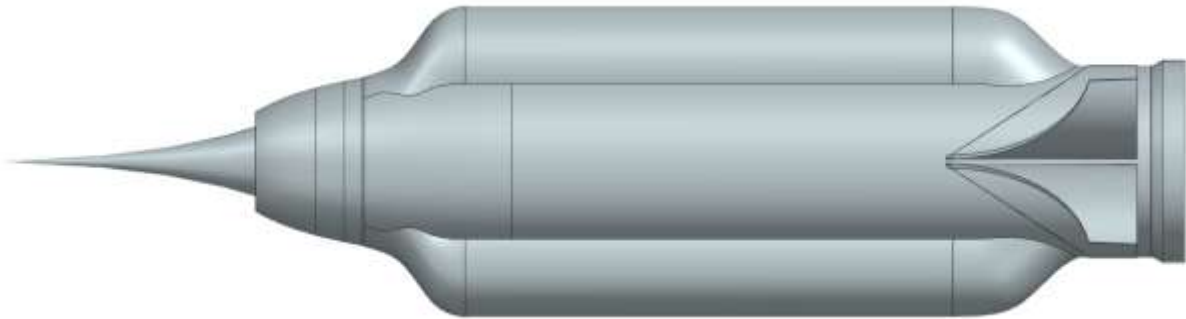


Figure 6.14: Top View of the 105mm RAIDER in the Terminal Configuration

Figure 6.15 shows a cutaway view of the internals of the projectile in this configuration. Key details are labeled, including deployed control surfaces and ducts, and the ramjet engine inlet, throat, combustion chamber, and nozzle.

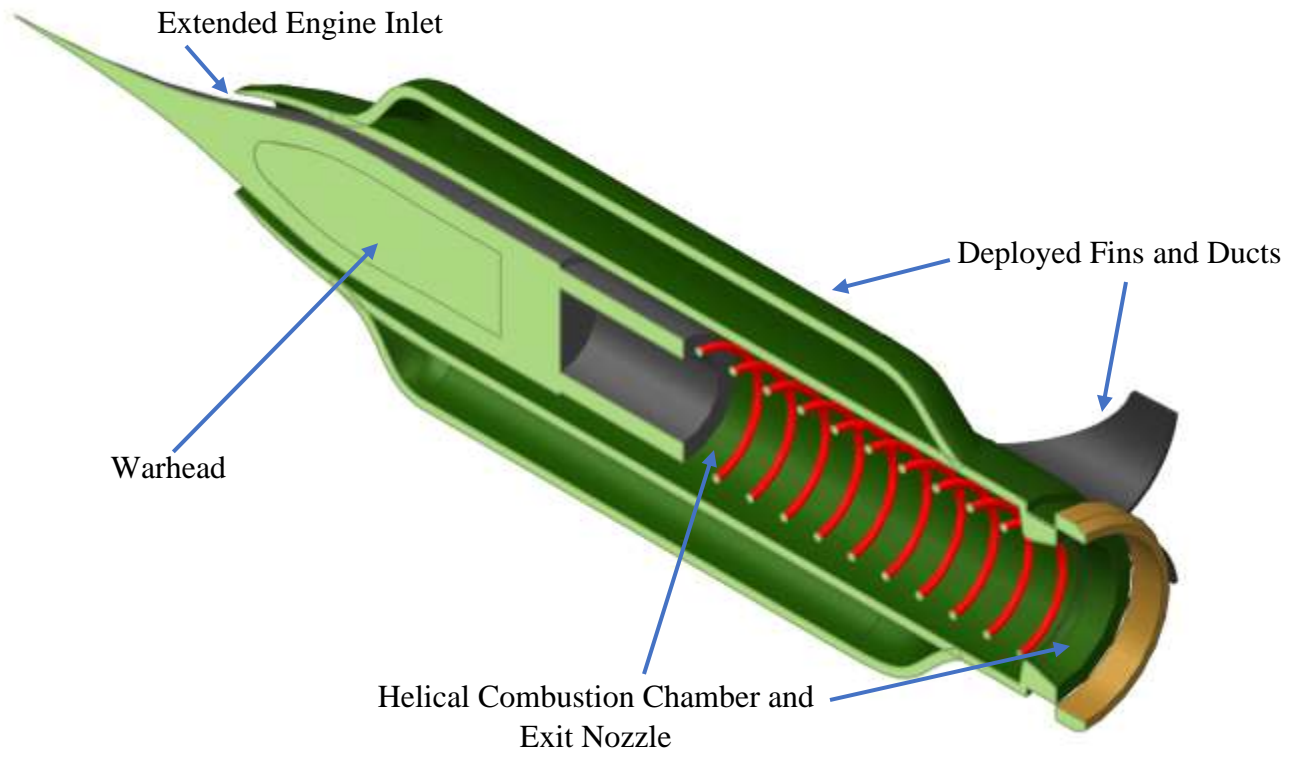


Figure 6.15: Isometric Cutaway View of the 105mm RAIDER in the Terminal Configuration

7 Conclusions and Recommendations

7.1 Summary

Relevant technical data for the 105mm RAIDER is provided in Table VIII below.

Table VIII: 105mm RAIDER Geometric and Salient Characteristics

Characteristic	Measurement
Projectile Length	24.212 in.
Nose Length	12.441 in.
Nose Diameter	0.039 in.
Fin Mean Aerodynamic Chord	0.228 in.
Fin Total Surface Area	0.236 in.
Fin Leading Edge Sweep Angle	56.3 deg
Mean Aerodynamic Chord Thickness	0.091 in.
Wingspan Fin	3.937 in.
Leading Edge Section Angle	2 deg
Inlet Area	8 in ²
Inlet Throat Area	6.8 in ²
Combustor Area	15 in ²
Throat Area	0.45 in ²
Exit Area	7.1 in ²
Combustor Length	3.8ft
Combustor Temperature Ratio	11.7
Fuel Enthalpy	17900 BTU/lbm
Fuel Volume	22 in ³
Thrust	2.8 lbf
Thrust to Drag Ratio	1
Specific Impulse	256 s

Additional important notes about the 105mm RAIDER are included below:

- The nose acutates to provide optimal inlet and inlet throat areas during all flight phases, being retracted during launch and deployed for cruise flight,
- The RAIDER ducts are constructed of shape memory alloys, deploying after the projectile has reached apogee for cruise flight,
- The helical twist added to the combustion chamber allows the projectile to have an artificially long combustor length without additional footprint,
- The current fin configuration stabilizes the projectile in a manner that allows the projectile to make use of the RAIDER ducts to generate lift, thus increasing efficiency.

7.2 Recommendations

Based on the conclusions of this report, the authors recommend the following:

- Consider implementation of canards to enable more control authority, greater precision, and lower circular area probable,
- Continue to make iterations on the propulsion system to increase efficiency of the projectile during cruise flight,
- Redesign nose section to streamline design, reduce projectile footprint, and increase inlet efficiency at higher Mach numbers.

7.3 Section Responsibilities

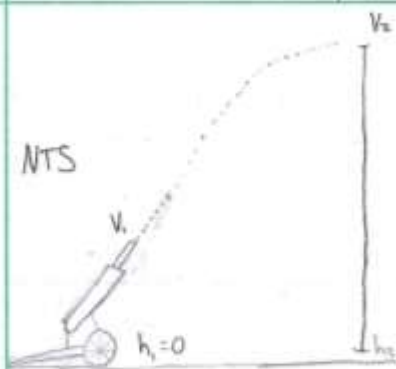
This section lists each team member along with the work they contributed to the report. This list only details primary responsibilities and does not cover any minor assistance or overlap that was experienced. (Verify again before submission).

- Joseph Atvie: Section 4
- Payton Kuligowski: Sections 1, 5, and 7
- Joshua Poznanski: Section 6
- Jakob Richardson: Section 3 and 6
- Cade Schneider: Sections 3 and 6
- Hector Torres: Sections 2 and 6

References

1. Ativie, J., Kuligowski, P., Poznanski, J., Richardson, J., Schneider, C., and Torres, H., “AE 721 Report 6: 105mm RAIDER Ammunition Benchmark and Aerodynamic Properties II, Reverse and Proverse Engineering,” University of Kansas Department of Aerospace Engineering, Lawrence, Kansas, 2023.
2. Fleeman, E. L., “Aerodynamic Considerations in the Missile Design and System Engineering Process,” *Missile Design and System Engineering*, 1st ed., Lilburn, Georgia, 2012, pp. 33 – 119.
3. Anon., “Gun Cartoon,” CleanPNG. Accessed 27 Nov 2023.
4. Anon., “Cartoon Explosion,” CleanPNG. Accessed 27 Nov 2023.

Appendix A: Calculation of Apogee Altitude



Ground Launch: $h_1 = 0$
 Assume Sea Level Conditions: $a \approx 1100 \text{ ft/s}$
 Assume 50% of muzzle KE lost at high altitude: $0.5 KE_1 = KE_2$
 Round Exits Muzzle @ Mach 7
 Reaches High Altitude @ Mach 4
 before RAIDER engagement

$$0.5 KE_1 + PE_1 = KE_2 + PE_2$$

$$0.5 \left(\frac{1}{2} m V_1^2 \right) + mg h_1 = \frac{1}{2} m V_2^2 + mg h_2$$

$$0.5 \left(\frac{1}{2} m V_1^2 \right) = \frac{1}{2} m V_2^2 + mg h_2 \rightarrow 0.5 \left(\frac{1}{2} V_1^2 \right) = \frac{1}{2} V_2^2 + g h_2$$

$$0.5 \left(\frac{1}{2} V_1^2 \right) - \frac{1}{2} V_2^2 = g h_2 \rightarrow \frac{0.5 V_1^2 - V_2^2}{2} = g h_2 \rightarrow h_2 = \frac{0.5 V_1^2 - V_2^2}{2g}$$

$$\text{Mach 7: } V = Ma \rightarrow V_1 = 7(1100 \text{ ft/s}) = 7700 \text{ ft/s}$$

$$\text{Mach 4: } V_2 = 4(1100 \text{ ft/s}) = 4400 \text{ ft/s}$$

$$h_2 = \frac{0.5(7700 \text{ ft/s})^2 - (4400 \text{ ft/s})^2}{2(32.2 \text{ ft/s}^2)} \rightarrow h_2 = \frac{10285000 \text{ ft}^2/\text{s}^2}{64.4 \text{ ft/s}^2} \rightarrow h_2 = 159704.97 \text{ ft}$$

$$h_2 \approx 160,000 \text{ ft}$$